Discover Environment

Research

The curing performances of lead-contaminated soil conditioned with modified phosphorus β-hemihydrate gypsum cemented materials

Xuquan Huang[1,2,3] · Ruting Wang[1,2,3] · Xiaorong Zhao[1,2,3] · Mingming Jiang[1,2,3] · Yunzhi Tan[4] · Haojie Wang[1,2,3]

Received: 17 October 2023 / Accepted: 28 February 2024

Abstract
A novel modified phosphorus β-hemihydrate gypsum (MPG) cementing material was developed to solidify lead-contaminated soil. The solidification effects of lead in the contaminated soil with MPG and Portland cement (PC) as curing agent were contrasted by the unconfined compressive strength (UCS), pH and leaching toxicity of solidified soil. The solidification mechanism of lead contaminated soil was analyzed by XRD, BET, SEM and EDS. The results demonstrated that when the addition of binder increased from 24 to 30%, the UCS of MPG solidified body became higher than that of PC solidified body by 14.7–18.8%. The pH of MPG solidified body was 9.81–10.69, which was 15.17–22.08% lower than that of PC solidified body. The lead leaching concentration of MPG solidified body decreased continuously with the curing time and became lower than the limit of hazardous waste content (5 mg L^{-1}) stipulated in Chinese standards after 7-day curing. The results of microscopic analysis revealed that the main components of MPG solidified body were ettringite (AFt), reticulated gel of calcium silicate hydrated (C–S–H), lead phosphate ($[Pb_{10}(PO_4)_6(OH)_2]$) and lead sulfate ($PbSO_4$) precipitation. The covering of C–S–H on soil particles and the ion exchange between lead and AFt contributed jointly to the stabilization of lead in the solidified soil. This is a valuable application exploitation study for the treatment of Pb contaminated soil and reutilization of waste phosphorus gypsum.

Keywords Modified phosphogypsum · Lead contaminated soil · Leaching · Heavy metal · Solidification/stabilization

1 Introduction

Heavy metal pollution of farmland soil has become one of the serious environmental problems threatening many countries in the world. According to the *Report on the National General Survey of Soil Contamination* (Ministry of Ecology and Environment, P.R. China, 2014), 16.1% of soil was polluted by various kinds of contaminants, among which the lead was the common heavy metal contaminant [1]. According to statistics, the current global average Pb enrichment rates are between 6 and 35 times background [2]. Human activities, such as the abuse of pesticide, discharge

---

✉ Xiaorong Zhao, rongrong315@ctgu.edu.cn; Xuquan Huang, hxq@ctgu.edu.cn; Ruting Wang, 202108150021029@ctgu.edu.cn; Mingming Jiang, 36006@ccepc.com; Yunzhi Tan, yztan@ctgu.edu.cn; Haojie Wang, whj2023060@ctgu.edu.cn | [1]Engineering Research Center of Eco-environment in Three Gorges Reservoir Region, Ministry of Education, China Three Gorges University, Yichang 443002, People's Republic of China. [2]College of Hydraulic & Environmental Engineering, China Three Gorges University, Yichang 443002, People's Republic of China. [3]Yichang Key Laboratory of Solid Waste Disposal and Resource Utilization (China Three Gorges University), Yichang 443002, People's Republic of China. [4]Key Laboratory of Geological Hazards On Three Gorges Reservoir Area of Ministry of Education, China Three Gorges University, Yichang 443002, People's Republic of China.

Discover Environment (2024) 2:29 | https://doi.org/10.1007/s44274-024-00046-0

of industrial wastewater, smelting, traffic emissions, mining and sewage irrigation, cause the wide distribution of lead in the soil [3–5]. Excessive lead in soil will not only change the physical and chemical characteristics of soil and pollute the surrounding air and water environment [6], but also seriously harm human health through the food chain. For example, even low concentrations of lead can cause acute and chronic diseases of various organ systems, such as anemia, hypertension and cardiovascular diseases [7]. Because of its damage to the soil ecosystem and human health, lead has been identified as one of major public health concerns by the World Health Organization (WHO) [8], therefore the restoration of lead-contaminated soil urgently needs to be addressed.

Solidification/stabilization (S/S) technology has been widely used in the remediation of heavy metal contaminated soil because of its low cost, easy implementation and immediate efficiency [9, 10]. S/S technology stabilizes heavy metals by various chemical reactions between different curing agents and heavy metals to adsorb or form precipitate heavy metal ions [11–13]. Ordinary Portland cement (PC) is a popular curing agent used in S/S technology, but it also has some limitations such as high energy consumption and 5–10% emission of global anthropogenic CO_2 [14]. At the same time, PC is hard to be used in treating soil polluted with high concentration of heavy metals, and easy to induce some problems such as poor durability and instability of the conditioned soil [15, 16]. Therefore, more and more researches focus on the development of new environmentally friendly curing agents, including industrial solid wastes such as alkali slag, steel slag, blast furnace slag and phosphogypsum (PG) as curing agents. An et al. [17] explored the performance of alkali residue mixed cement as curing agent to stabilize lead-contaminated soil and the results showed that the lead concentration of leachate from solidified body with pure cement as the curing agent was about three times that with alkali residue mixed cement. Bashir et al. [18] studied the effect of steel slag on the leaching behavior and chemical form of Cd in Cd-contaminated soil through column leaching test and found that steel slag transformed Cd in soil into stable precipitation form through precipitation and adsorption. Safa et al. [19] combined MgO-activated basic oxygen furnace (M-BOF) slag with polypropylene fiber to solidify Zn/Pb contaminated soil and found that the frost durability in the M-BOF/fiber specimens appears to be about 3.5 times higher than that of those with only PC. Komaei et al. [20] studied the potential of alkaline activated slag for stabilization and solidification of arsenic-contaminated soil and discovered that alkaline activated slag promoted the formation of geopolymer gels based on calcium and silica, which was helpful to improve the mechanical strength of solidified body and reduce the leaching rate. Wang et al. [21] used blast furnace slag to prepare compound binder, which effectively immobilized lead in sludge polluted by heavy metals. Reddy et al. [22] prepared a new ternary blend manufactured by the replacement of 50% cement clinker with limestone and calcined clay for stabilization of Zn-contaminated soil, overcoming the interference of Zn on cement hydration and retardant effects. Wang et al. [23] studied the solidification effect of red mud phosphogypsum coupled Portland cement on polymetallic contaminated soil and the results showed that the soil strength of stabilized body could meet the strength requirements of landfill and the leaching concentration of metal could meet the standard of hazardous waste in China.

PG is an industrial waste from the wet production process of phosphoric acid, and the production of 1 ton of phosphoric acid would induced 4–6 tons of PG [24]. Calcium sulfate dihydrate ($CaSO_4 \cdot 2H_2O$) was the main component of PG [25]. The cumulative accumulation of PG in China is about 500 million tons, and has been increasing rapidly at the rate of 55 million tons per year [26]. The accumulation of PG not only occupies a large amount of land resources, but also pollutes the surrounding soil and water environment due to fluorine and phosphorus in the leachate of PG [27, 28]. Less than 15% of the total PG was put into multipurpose utilization as building gypsum, high strength gypsum, cement retarders and soil conditioners [29, 30]. Due to the existence of sulfate, PG can be used in combination with two typical industrial solid wastes, namely slag and phosphorus slag. Cement clinker or lime is added as alkaline activator, and a curing agent with hydraulic property is generated through pozzolanic reactions for solidify/stabilize heavy metal contaminated soil. Compared with PC, this new curing agent is more conducive to saving resources and protecting the environment. At the same time, due to the phosphate groups, PG can constitute an excellent adsorbent material, which is expected to form insoluble phosphate mineral phase and further immobilize heavy metal ions. Scheckel et al. [31] transformed the Pb ion in soil into insoluble Pb-phosphate (pyromorphite or tertiary lead phosphate) by adding phosphorus compounds to the soil for chemical fixation. Lamzougui et al. [32] concluded that PG could be used as an effective adsorbent to remove Pb from aqueous solution. Syczewski et al. [33] studied the sorption capacity of PG-ceramic composites for uranyl and the results showed that the addition of PG increased the adsorption capacity by chemical adsorption. Calcined phosphogypsum has much larger specific surface area than PG and some gel properties, therefore it is expected to improve the adsorption of heavy metal ions in polluted soil when coating the surface of soil particles. However, the high cost of high temperature for calcination severely restricted its widespread adoption in the remediation of contaminated soil, so it is an urgent issue to lower the calcination temperature of PG.

In this study, the contact point of $CaSO_4 \cdot 2H_2O$ crystal is increased by adding fly ash, slag and quicklime to PG, and the heat absorption rate is increased, so as to reduce the calcination temperature of PG. Then, the modified phosphorus β -hemihydrate gypsum cementitious material (MPG) prepared through low-temperature calcination was fabricated to solidify the lead in contaminated soil. The solidification effect of lead in the contaminated soil with MPG as curing agent was explored by the unconfined compressive strength (UCS), pH and leaching toxicity of solidified soil. The solidification mechanism of lead contaminated soil was analyzed by XRD, BET, SEM and EDS. This study is a powerful exploration for the reutilization of industrial waste PG and simultaneous remediation of lead-contaminated soil, and the results could provide an economical and effective environment-friendly curing agent for the solidification of lead-contaminated soil.

2 Material and methods

2.1 Experiment materials

Phosphorus β-hemihydrate gypsum (PHG) was prepared by uniformly mixed PG, fly ash (FA), slag (GS) and quicklime (QL), according to the ratio of 91:3:4:2, calcining at 170 ℃ for 2.5 h, and then cooling in a dryer to room temperature, in which PG needs to be dried at a low temperature of 45 ℃, and then mechanically ground and screen with a sieve of 1 mm for later use. The MPG was fabricated by adding GS, phosphorus slag (PS) and clinker (CC) into PHG doped with additional 2.5% (wt%) QL as alkali-activator and the mass percentage of PHG: GS: PS: CC was set as 51.4%:23.9%:14.7%:10% [34]. The main chemical composition (mass percentage, wt%) of PG, GS, FA, PS, PC and CC are shown in Table 1. The QL (CaO% ≥ 89.8%) was from Hubei Magic Red Stone Industry Company.

The soil used in this work was silty clay with low liquid limit taken from the suburbs of Yichang City, and the main physicochemical indexes were shown in Table 2. Lead nitrate ($Pb(NO_3)_2$) was used as the lead pollution source to simulate lead-contaminated soil (8000 mg/kg, 0.8%). Mixed lead nitrate with deionized water, subsequently stirred with a magnetic stirrer for 5 min to thorough dissolution, poured the solution into silty clay and mechanically stirred it for 5 min, then sealed the mixture for 48 h to make lead nitrate fully contact with soil particles, finally the acquired product was simulated lead-contaminated soil.

2.2 Test method

2.2.1 Sample preparation and unconfined compressive strength test

In this study, when the lead-contaminated soil was stabilized with MPG and PC, respectively, the resulted solidified bodies were noted as MPG-Pb and PC-Pb, respectively. The employed dosage of curing agent accounts for 6%, 12%, 18%, 24% and 30% of the dry weight of lead-contaminated soil, respectively. According to the proportion, the curing agent and the lead-contaminated soil are stirred to prepare a 40 mm cube, which is cured at 20 ± 1 ℃ and humidity greater than 95% for 48 h. After demoulding, it was put into a standard curing box for curing to the specified age. Compressive strength test was carried out according to the physical and mechanical performance requirements of *"Building Gypsum"* (GB/T 9776-2008).

Table 1 Main components of the materials

Material	CaO	SiO_2	Al_2O_3	MgO	SO_3	Fe_2O_3	P_2O_5	K_2O	Na_2O	F
PG	37.75	8.29	0.86	0.08	50.59	0.58	1.27	0.52	0.06	0.28
GS	38.65	29.9	15.94	7.98	3.74	1.18	0.03	0.62	0.34	–
FA	4.63	45.06	39.06	0.66	0.71	3.98	0.32	0.98	0.59	–
PS	42.47	40.56	5.38	1.32	1.34	0.60	3.54	1.38	0.37	–
cement	43.67	28.39	10.32	6.62	2.17	2.64	–	–	–	–
CC	2.72	48.3	24.48	0.42	1.54	12.46	–	0.43	0.26	–

Table 2 Main physicochemical indexes of soil

Soil index	Optimum moisture w_m (%)	Plastic limit w_p (%)	Liquid limit w_L (%)	Maximum dry density $\rho_{d/}$(g cm^{-3})	Organic matter (%)	pH
Silty clay	15.12	18	32	1.93	0.23%	7.77

2.2.2 Test of pH and leaching toxicity

The differences of pH between MPG-Pb and PC-Pb were studied. Take the middle part of the solidified sample to dry at 35 ℃ and cool, subsequently grind, finally screen with a sieve of 1 mm. A portion of soil and five portions of deionized water were mixed together for five minutes. After standing for 30 min, the pH value of soil suspension was detected with a precision acidity meter [35].

The lead leaching performances of solidified lead-contaminated soil were evaluated according to the environmental safety standards. The test of leaching toxicity was carried out referring to "*Identification standards for hazardous wastes-Identification for extraction toxicity*" (GB5085.3-2007) with the lead leaching limit as 5 mg L^{-1}. The leaching test was carried out according to "*Solid waste-Extraction procedure for leaching toxicity-Acetic acid buffer solution method*" (HJ/300-2007). Firstly, 5.7 mL glacial acetic acid and deionized water were mixed and dissolved into a 1 L volumetric flask to prepare the extractant with pH as 4.93 ± 0.05. Then sample 50 g solidified body, mechanically grind and sieve it (2 mm), put it with extractant into a polyethylene bottle according to the ratio of 20:1 (g: L), then fix the polyethylene bottle in a water bath shaker with a thermostat (23 ± 2 °C) for vibrating horizontally for 18 ± 2 h. After 16 h settling, the supernatant was taken out to centrifuge for 10 min. The lead concentration in the leaching was analyzed according to "*Solid waste—Determination of Lead, Zinc and Cadmium—Flame Atomic Absorption Spectrometry*" (HJ786-2016). Analyze each leaching sample three times with a relative deviation less than 1.56%.

2.2.3 Structural and microscopic characterization

After the UCS test was completed, the broken sample was immersed into absolute ethanol for 48 h to terminate the hydration reaction and put into a 35 ℃ oven to dry until constant weight. The chemical element types and mass percentages on the surface of the hydration products in the sample were identified by JSM-IT300 scanning electron microscope (SEM) combined with energy dispersive spectroscopy (EDS).

The dried samples were further ground and sieved (200 mesh), and the sieved samples were scanned by X-ray diffraction (XRD). The Rigaku Ultima IV diffractometer with Cu target was used to scan in the range of 2θ from 5 to 80 degree at a speed of 2° min^{-1} to qualitatively evaluate the types of mineral phases. Specific surface area (BET) test was carried out with a specific surface area and aperture analyzer.

3 Results and discussion

3.1 Unconfined compressive strength

Figure 1a presented the 28-day UCS of lead-contaminated silty clays solidified with different dosages of MPG and PC. The UCS of uncured lead-contaminated silty clays was zero MPa. With the increase of curing agent dosage, the UCS of the cured body increases in a power function (Fig. 1a). The results of polynomial curves fitting of UCS (y) *vs.* binder dosage (x) for MPG-Pb and PC-Pb were $y = -1.32 + 0.142x + 0.00875x^2$ ($R^2 = 0.993$) and $y = -0.818 + 0.203x + 0.00417x^2$ ($R^2 = 0.997$), respectively. This shows that the increase of MPG dosage contributes more to the improvement of UCS than that of PC

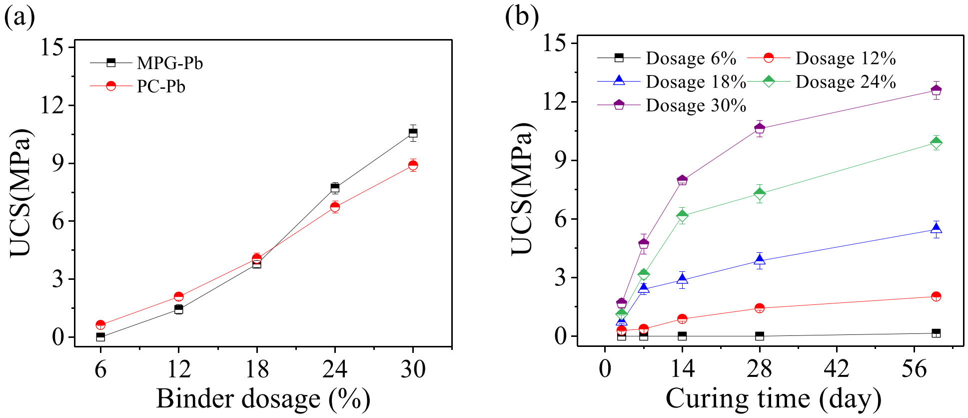

Fig. 1 **a** The UCS of solidified body with different binders and **b** effect of different dosages on the UCS of MPG solidified body at different periods

dosage. When the dosage of binder increased from 6 to 18%, the UCS of MPG solidified body was lower than that of PC solidified body, and the difference of UCS decreases with the increase of curing age. When the addition of binder increased from 24 to 30%, the UCS of MPG solidified body became higher than that of PC solidified body by 14.7–18.8%.

Figure 1b shows the UCS of MPG cured body with different dosages at different curing periods. At the same period, the UCS of MPG solidified body increased with the increase of curing agent dosage. The UCS of MPG cured body increased rapidly in the initial stage of curing (7–28 days) and continued to increase in the later stage of curing (28–60 days). These findings verified that the UCS of MPG solidified body increased with the extension of curing age [36, 37].

3.2 pH and leaching toxicity test

The pH of lead contaminated soil was 6.45, while that of MPG and PC was 11.3 and 11.8, respectively, which was helpful to improve the alkalinity of solidified soil. According to Fig. 2a, the pH value of MPG-Pb was less than that of PC-Pb by 15.17%-22.08%. This is because the hydration and hardening of MPG-Pb consumes $Ca(OH)_2$, while that of PC-Pb generates $Ca(OH)_2$, making the pH value higher. The lead concentration in leaching of unsolidified body reached 11.35 mg L^{-1} (Fig. 2b), being 2.27 times of the national lead toxicity leaching limit of hazardous solid waste (5.0 mg L^{-1}, GB 5085.3-2007). When the dosage of MPG was 24% and 30%, respectively, the lead concentration in leaching of solidified body declined to 1.42 and 0.7 at the initial curing stage (7–28 days), to 0.37 and 0.01 at the later curing stage (28–180 days), being lower than the safety limit of 5 mg L^{-1}. It can be seen that the lead concentration in leaching of cured body decreased rapidly with the increase of curing age in the early period (7–28 days), and tended to be stable in the later stage (28–180 days). The mechanism of MPG curing Pb(II) will be discussed in Sects. 3.3, 3.4, 3.5.

3.3 XRD analysis

Silica (SiO_2), calcite ($CaCO_3$) and anorthite ($CaAlSi_3O_8$) were the main solid mineral phase of undisturbed clay (Fig. 3a). The solid mineral phase of the MPG-Pb included AFt, lead sulfate, lead hydroxyphosphate and calcium sulfate dihydrate. As the curing age increases, the diffraction peak of AFt intensifies gradually, indicating the continuous growth in the amount of AFt in the solidified body. AFt crystals cross-filled in the inner pores of solidified body, reduced the porosity of solidified body [38, 39] and therefore improved the structural stability and compactness of the cured body.

The detection of lead sulfate ($PbSO_4$) indicated that when MPG solidified lead pollution, phosphorus β-hemihydrate gypsum dissolved into calcium sulfate dihydrate ($CaSO_4 \cdot 2H_2O$) gel with large specific surface area, and part of Pb(II) in soil replaced Ca^{2+} in $CaSO_4$, resulting in the precipitation of $PbSO_4$. Meanwhile, phosphate anion (PO_4^{2-}) and Pb(II) formed insoluble lead phosphate minerals [40, 41], which weakened the dissolvability and migration of lead [42].

3.4 Solidified body pore analysis

The adsorption–desorption isotherms in Fig. 4a were the type II isotherm, indicating that the adsorption on the surface of macroporous solids was multi-molecular layer adsorption. The adsorption–desorption curve of the MPG solidified body was located under that of PC solidified body, indicating that the adsorption capacity of N_2 on the MPG solidified body was less than that on the PC solidified body, and the pore volume was smaller than that of the PC solidified body. Figure 4b shows that the cumulative pore volume in the MPG solidified body with a pore

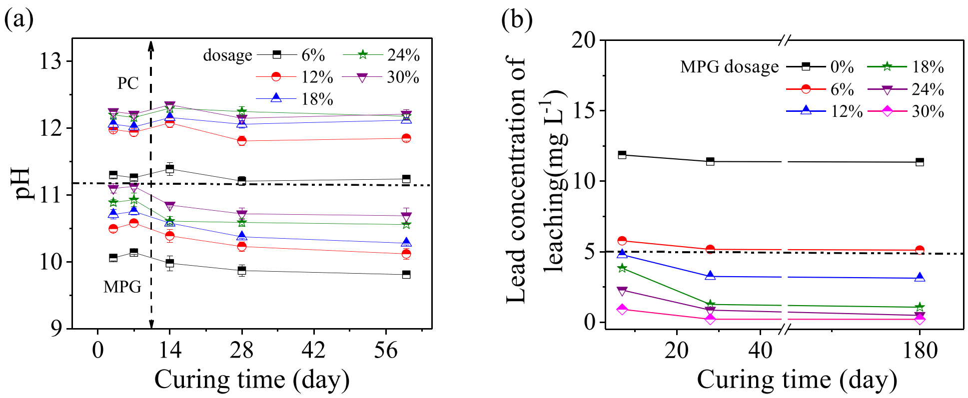

Fig. 2 **a** pH of solidified body with MPG and PC and **b** lead concentration of leaching of lead-contaminated soil solidified by MPG of different dosages

Fig. 3 X-ray diffraction patterns of **a** original soil and MPG solidified body at curing age of **b** 7 days, **c** 28 days and **d** 180 days

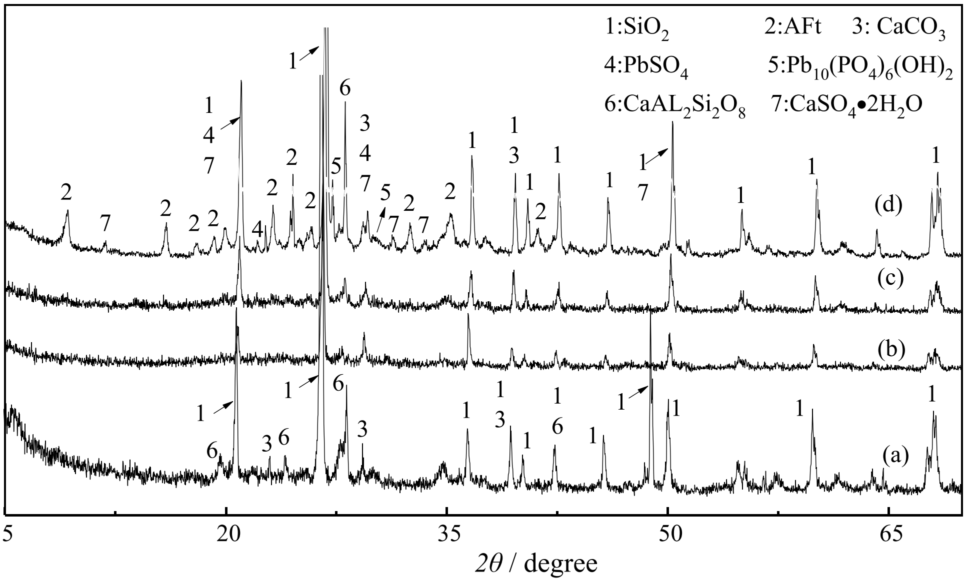

Fig. 4 **a** Isothermal adsorption–desorption curve, **b** cumulative pore volume and **c** distribution of differential aperture of 28-day stabilized lead-contaminated soil specimens with MPG and PC as binder, respectively

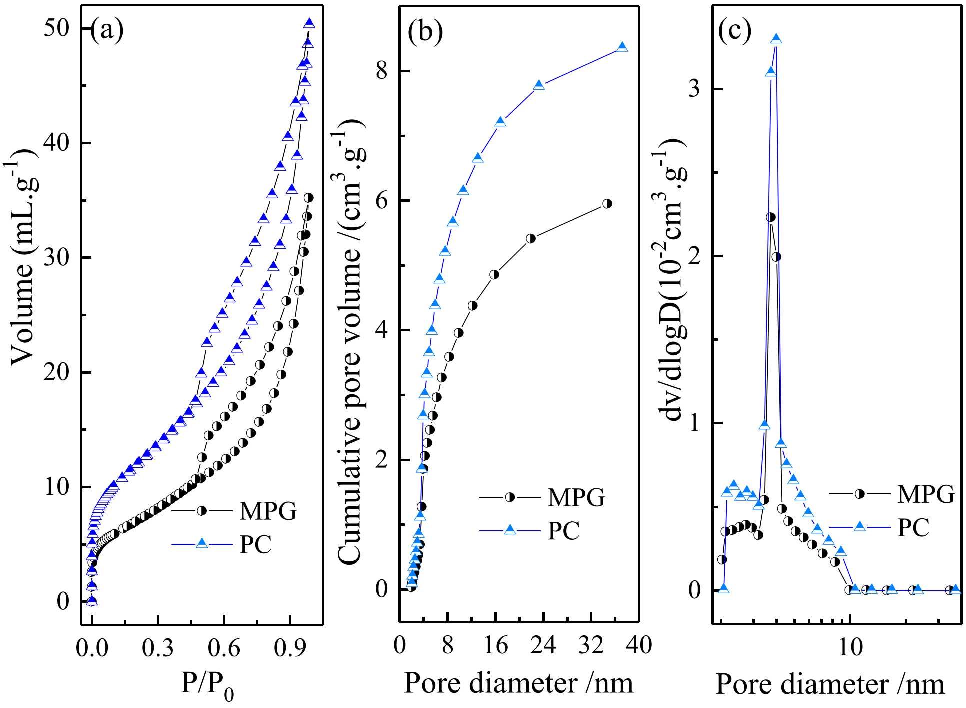

diameter over 5.0 nm was significantly less than that of PC solidified body. These results indicated that the amount of macropores in MPG solidified body was less than that of PC solidified body, but macropores were easy to form feed-through, which could increase Pb(II) leaching property [43], therefore MPG solidified body was more conducive to lead solidification and stability. From the differential aperture distribution curve (Fig. 4c), an obvious characteristic peak appeared at 4.0 nm or so for MPG and PC solidified body, respectively, and the pore diameter distribution of the MPG solidified body was beneath that of the PC solidified body, revealing that the porosity of MPG solidified body was much weaker than that of PC solidified body. Low porosity usually means high structure density. Based on the above discussion, it is clear that the strength in macroscopic properties of MPG solidified body was higher than that for PC solidified body, which reconfirmed the test result of UCS in Sect. 3.1.

3.5 SEM characteristic

Figure 5a and b presented the difference in micromorphology between MPG solidified body and PC solidified body at different magnification scales after 28-day curing. Figure 5a showed the difference of hydration products between them. It can be seen that MPG solidified body has a large number of pin-like ettringite crystals (AFt) and reticular C–S–H gel, and AFt was cross-filled in the pores between soil particles to support a stable framework structure. The C–S–H gel of network structure covered the surface of soil particles and AFt crystals, increased the cementation between soil particles and therefore enhanced the strength of the solidified body [44]. The hydration product of C–S–H gel has a large specific surface area and strong adsorptivity. Pb(II) in soil was adsorbed onto the hydration product of gel surface, which played a role in the stabilization of Pb(II) [45, 46] to reduce the solubility and migration of Pb(II). Many hydration products of C–S–H gel and hexagonal flakes calcium hydroxide appeared in the PC solidified body and the presence of calcium hydroxide was the main resource of high alkalinity. Neither needle-like nor thin rod-like AFt crystals was observed in PC solidified body. The absence of filling effect of AFt crystals between the soil particles contributed to the formation of through hole and increased the leaching probability of Pb(II). The internal pore size of MPG and PC solidified body was contrasted in Fig. 5b. It was found that the porous hydration product of MPG solidified soil spread over the entire area of the solidified body with a great number of small pores and good compactness. Compared with that in MPG solidified soil, the number of large pores in PC solidified body was obviously much more, inducing that the macroscopic performance, compactness and intensity of PC solidified soil was lower than that of MPG solidified soil.

The main elements detected in the solidified body were oxygen, calcium, aluminum and silicon (Fig. 6), which correspond to the main hydration products C–S–H, AFt, C–A–H and SiO_2, respectively. The detected content of Pb element in MPG solidified body was 6.27%, which was 1.83 times that of PC solidified body, indicating that the number of lead-containing minerals generated on the surface of hydration products of MPG solidified body was more than that of PC. Phosphorus and sulfur were also detected in MPG solidified body, but not in PC solidified body, which may be because their contents were lower than the detection limit of the instrument. The phosphorus and sulfur elements detected in MPG solidified body demonstrated the formation of lead phosphate and lead sulfate minerals, but no similar minerals were found in PC solidified body. This result is in keeping with the above findings of XRD analysis, supporting that the formation of lead phosphate and lead sulfate precipitation was an important mechanism for MPG to solidify lead-contaminated soil [40, 47].

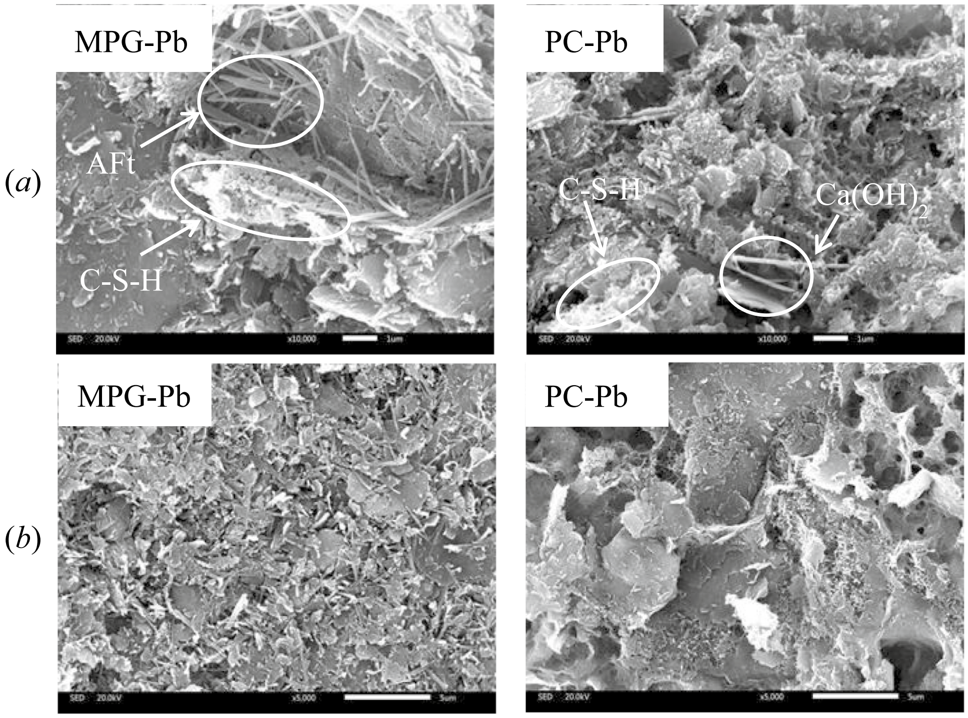

Fig. 5 SEM photos of MPG and PC solidified body

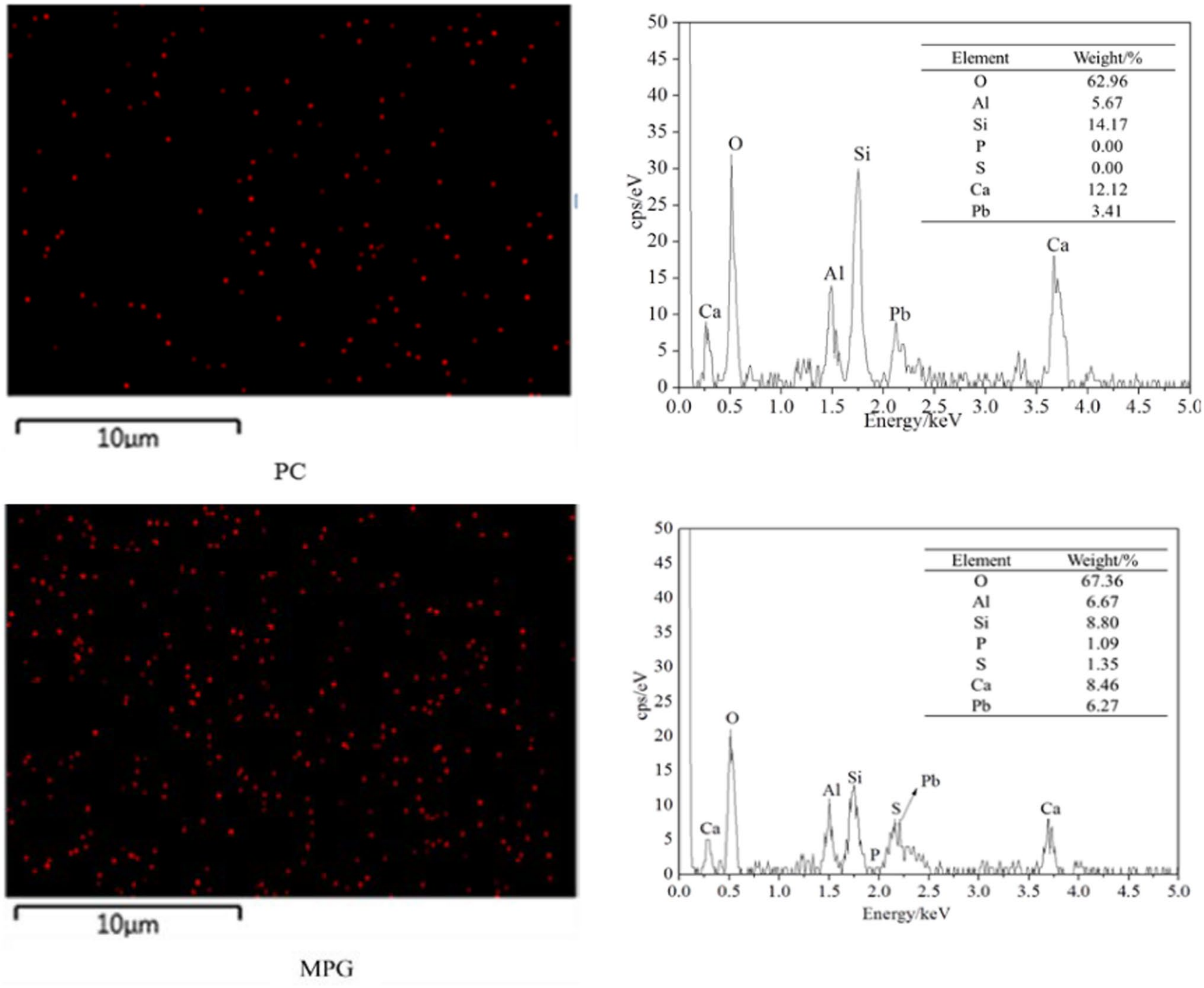

Element	Weight/%
O	62.96
Al	5.67
Si	14.17
P	0.00
S	0.00
Ca	12.12
Pb	3.41

Element	Weight/%
O	67.36
Al	6.67
Si	8.80
P	1.09
S	1.35
Ca	8.46
Pb	6.27

Fig. 6 SEM–EDS photos of MPG and PC solidified lead-contaminated soil

4 Conclusion

In this work, the solidification effect of MPG on lead-contaminated soil and its curing reaction mechanism were studied. The results proved the effectiveness of MPG solidification on lead-contaminated soil. Following are some of the specific findings of this work:

The test of pH indicated that MPG solidified lead contaminated soil could reduce acidity and alkalinity. Compared with PC, MPG greatly improved the UCS of solidified soil with the binder dosage over 24%, meanwhile, the leaching lead concentration reached the regulatory limit (5 mg L^{-1}) stipulated in Chinese standards, indicating the structural stability and chemical stability of MPG solidified body. Microscopic analysis presented that the hydration and hardening of MPG solidified body produced AFt for filling the soil pores, $PbSO_4$ and $[Pb_{10}(PO_4)_6(OH)_2]$ precipitates, cooperating with reticular C–S–H to fix lead in polluted soil and improve the mechanical strength. As expected, our study confirmed that MPG could be used as a curing agent for solidifying lead-contaminated soil, and it is also expected to be used for the remediation of other heavy metal-contaminated soils. The use of MPG can also reduce the environmental problems caused by the stockpiling of industrial solid wastes such as PG, promoting circular economy and reducing emission of greenhouse gases, and at the same time provides a competitive way to prepare green curing agent from industrial solid waste for the treatment of lead-contaminated soil. In addition, this study aimed at the indoor study of silty clay, and it is necessary to study the applicability of other types of contaminated soil in engineering practice to increase the application scenarios of MPG.

Acknowledgements This work was financially supported by Natural Science Foundation of Yichang (A21-3-003 and A23-2-020) and Open Research Program of Engineering Research Center of Eco-environment in Three Gorges Reservoir Region, Ministry of Education (KF2022-11 and KF2023-07). All authors express our sincere gratitude for your support.

Author contributions All authors contributed to the study conception and design. This research was conceived and designed by XH. Material preparation, data collection and analysis were performed by RW, MJ, YZ, and HW. The first draft of the manuscript was written by RW, and all authors commented on previous versions of the manuscript. Conceptualization, resources, writing—reviewing and editing by XZ. All authors read and approved the final manuscript.

Data availability All data generated or analyzed during this study are included in this published article.

Declarations

Ethical approval consent to participate Not applicable.

Consent for publication Not applicable.

Competing interests The authors declare that they have no known competing financial interests or personal relationships that could have appeared to influence the work reported in this paper.

References

1. Ren S, et al. The spatiotemporal variation in heavy metals in China's farmland soil over the past 20 years: a meta-analysis. Sci Total Environ. 2022;806:150322. https://doi.org/10.1016/j.scitotenv.2021.150322.
2. Marx SK, et al. Global-scale patterns in anthropogenic Pb contamination reconstructed from natural archives. Environ Pollut. 2016;213:283–98. https://doi.org/10.1016/j.envpol.2016.02.006.
3. Gui H, et al. Spatial distribution, contamination characteristics and ecological-health risk assessment of toxic heavy metals in soils near a smelting area. Environ Res. 2023;222:115328. https://doi.org/10.1016/j.envres.2023.115328.
4. Zhang Y, et al. Pollution assessment and source apportionment of heavy metals in soil from lead–Zinc mining areas of south China. J Environ Chem Eng. 2023;11(2):109320. https://doi.org/10.1016/j.jece.2023.109320.
5. Xu Z, et al. Characteristics and sources of heavy metal pollution in desert steppe soil related to transportation and industrial activities. Environ Sci Pollut Res. 2020;27(31):38835–48. https://doi.org/10.1007/s11356-020-09877-9.
6. Moghal AAB, et al. Leaching test protocols to evaluate contaminant response of nano-calcium silicate-treated tropical soils. J Hazard Toxic Radioact Waste. 2023;27(2):04023002. https://doi.org/10.1061/JHTRBP.HZENG-1200.
7. Lanphear BP, et al. Low-level lead exposure and mortality in US adults: a population-based cohort study. Lancet Public Health. 2018;3(4):e177–84. https://doi.org/10.1016/S2468-2667(18)30025-2.
8. Dobrescu A-I, et al. Effectiveness of interventions for the remediation of lead-contaminated soil to prevent or reduce lead exposure—a systematic review. Sci Total Environ. 2022;806:150480. https://doi.org/10.1016/j.scitotenv.2021.150480.
9. Ma Y, et al. Stabilization and remediation of heavy metal-contaminated soils in China: insights from a decade-long national survey. Environ Sci Pollut Res. 2022;29(26):39077–87. https://doi.org/10.1007/s11356-021-18346-w.
10. Liu L, et al. Remediation techniques for heavy metal-contaminated soils: principles and applicability. Sci Total Environ. 2018;633:206–19. https://doi.org/10.1016/j.scitotenv.2018.03.161.
11. Jiang Q, et al. Solidification/stabilization of soil heavy metals by alkaline industrial wastes: a critical review. Environ Pollut. 2022;312:120094. https://doi.org/10.1016/j.envpol.2022.120094.
12. Ouhadi VR, et al. Enhancement of cement-based solidification/stabilization of a lead-contaminated smectite clay. J Hazard Mater. 2021;403:123969. https://doi.org/10.1016/j.jhazmat.2020.123969.
13. Moghal AAB, et al. Desorption of heavy metals from lime-stabilized arid-soils using different extractants. Int J Civ Eng. 2020;18(4):449–61. https://doi.org/10.1007/s40999-019-00453-y.
14. Dung NT, Unluer C. Carbonated MgO concrete with improved performance: the influence of temperature and hydrati-on agent on hydration, carbonation and strength gain. Cem Concr Compos. 2017;82:152–64. https://doi.org/10.1016/j.cemconcomp.2017.06.006.
15. Wang Y-S, et al. Influence of lead on stabilization/solidification by ordinary Portland cement and magnesium phosphate cement. Chemosphere. 2018;190:90–6. https://doi.org/10.1016/j.chemosphere.2017.09.114.
16. Provis JL, et al. Advances in understanding alkali-activated materials. Cem Concr Res. 2015;78:110–25. https://doi.org/10.1016/j.cemconres.2015.04.013.

17. An X, et al. Investigation on stabilization/solidification characteristics of lead-contaminated soil using innovative composite model of cement and soda residue. Environ Earth Sci. 2022;81(21):508. https://doi.org/10.1007/s12665-022-10629-w.
18. Bashir S, et al. Effective role of biochar, zeolite and steel slag on leaching behavior of Cd and its fractionations in soil column study. Bull Environ Contam Toxicol. 2019;102(4):567–72. https://doi.org/10.1007/s00128-019-02573-6.
19. Safa M, et al. Enhanced post freeze-thaw stability of Zn/Pb co-contaminated soil through MgO-activated steel slag and fiber treatment. Cold Reg Sci Technol. 2023;210:103826. https://doi.org/10.1016/j.coldregions.2023.103826.
20. Komaei A, et al. Stabilization and solidification of arsenic contaminated silty sand using alkaline activated slag. J Environ Manage. 2023;344:118395. https://doi.org/10.1016/j.jenvman.2023.118395.
21. Wang Y, et al. Strength and leaching behavior of heavy metal contaminated sludge solidified/stabilized by compound binders. Environ Res. 2021;197:111053. https://doi.org/10.1016/j.envres.2021.111053.
22. Reddy VA, et al. New ternary blend limestone calcined clay cement for solidification/stabilization of zinc contaminated soil. Chemosphere. 2019;235:308–15. https://doi.org/10.1016/j.chemosphere.2019.06.051.
23. Wang F, et al. Sustainable stabilization/solidification of the Pb, Zn, and Cd contaminated soil by red mud-derived binders. Environ Pollut. 2021;284:117178. https://doi.org/10.1016/j.envpol.2021.117178.
24. Qin X, et al. Resource utilization and development of phosphogypsum-based materials in civil engineering. J Clean Prod. 2023;387:135858. https://doi.org/10.1016/j.jclepro.2023.135858.
25. Rashad AM. Phosphogypsum as a construction material. J Clean Prod. 2017;166:732–43. https://doi.org/10.1016/j.jclepro.2017.08.049.
26. Chuan LM, et al. Phosphogypsum production and utilization in China. IOP Conf Ser Mater Sci Eng. 2018;382(2):022099. https://doi.org/10.1088/1757-899X/382/2/022099.
27. Tayibi H, et al. Environmental impact and management of phosphogypsum. J Environ Manage. 2009;90(8):2377–86. https://doi.org/10.1016/j.jenvman.2009.03.007.
28. Wang C-q, et al. Characteristic pollutant purification analysis of modified phosphogypsum comprehensive utilization. Environ Sci Pollut Res. 2022;29(44):67456–65. https://doi.org/10.1007/s11356-022-22737-y.
29. Cánovas CR, et al. Valorization of wastes from the fertilizer industry: current status and future trends. J Clean Prod. 2018;174:678–90. https://doi.org/10.1016/j.jclepro.2017.10.293.
30. Chen W, et al. Utilization of high-volume phosphogypsum in artificial aggregate by compaction granulation: effects of muck on physical properties, strength and leaching stability. J Sustain Cem-Based Mater. 2023;12(8):951–61. https://doi.org/10.1080/21650373.2022.2141368.
31. Scheckel KG, et al. Amending soils with phosphate as means to mitigate soil lead hazard: a critical review of the state of the science. J Toxicol Env Health-Pt B-Crit Rev. 2013;16(6):337–80. https://doi.org/10.1080/10937404.2013.825216.
32. Lamzougui G, et al. Optimization and modeling of Pb(II) adsorption from aqueous solution onto phosphogypsum by a-pplication of response surface methodology. Phosphorus Sulfur Silicon Relat Elem. 2021;196(6):521–9. https://doi.org/10.1080/10426507.2020.1860985.
33. Syczewski MD, et al. Phosphogypsum and clay mineral/phosphogypsum ceramic composites as useful adsorbents for uranium uptake. Appl Geochem. 2020;123: 104793. https://doi.org/10.1016/j.apgeochem.2020.104793.
34. Jiang M, et al. Research on the preparation of β-hemihydrate phosphogypsum at low temperature and properties of so-lidificed lead contaminated soils. Environ Pollut Control. 2019;41(04):402–6. https://doi.org/10.15985/j.cnki.1001-3865.2019.04.006.
35. Bao S. Soil agrochemical analysis. 3rd ed. Beijing: China Agricultural Publishing House; 2000.
36. Huang X, et al. Mechanical properties and hydration mechanisms of high-strength fluorogypsum-blast furnace slag-based hydraulic cementitious binder. Constr Build Mater. 2016;127:137–43. https://doi.org/10.1016/j.conbuildmat.2016.09.152.
37. Suo C, et al. Influence and microscopic mechanism of the solid waste-mixture on solidification of Cu^{2+}-contaminated soil. Constr Build Mater. 2021;305:124651. https://doi.org/10.1016/j.conbuildmat.2021.124651.
38. Whittaker M, et al. The role of the alumina content of slag, plus the presence of additional sulfate on the hydration and microstructure of Portland cement-slag blends. Cem Concr Res. 2014;66:91–101. https://doi.org/10.1016/j.cemconres.2014.07.018.
39. Zajac M, et al. Influence of limestone and anhydrite on the hydration of Portland cements. Cem Concr Compos. 2014;46:99–108. https://doi.org/10.1016/j.cemconcomp.2013.11.007.
40. Ren Z, et al. Solidification/stabilization of lead-contaminated soils by phosphogypsum slag-based cementitious materials. Sci Total Environ. 2023;857:159552. https://doi.org/10.1016/j.scitotenv.2022.159552.
41. Mozgawa W, et al. Application of IR spectra in the studies of heavy metal cations immobilization on natural sorbents. J Mol Struct. 2009;924–926:427–33. https://doi.org/10.1016/j.molstruc.2008.12.028.
42. Endovitsky AP, et al. Ions association in soil solution as the cause of lead mobility and availability after application of phosphogypsum to chernozem. J Geochem Explor. 2017;182:185–92. https://doi.org/10.1016/j.gexplo.2016.08.018.
43. Vočka R, et al. Mercury intrusion porosimetry and hierarchical structure of cement pastes: theory and experiment. Cem Concr Res. 2000;30(4):521–7. https://doi.org/10.1016/S0008-8846(99)00252-5.
44. Chen L, et al. Review on stabilization/solidification methods and mechanism of heavy metals based on OPC-based binders. J Environ Manage. 2023;332:117362. https://doi.org/10.1016/j.jenvman.2023.117362.
45. Żak R. Deja J Spectroscopy study of Zn, Cd, Pb and Cr ions immobilization on C–S–H phase. Spectrochim Acta Part A. 2015;134:614–20. https://doi.org/10.1016/j.saa.2014.06.069.
46. Yuan M, et al. In-situ remediation of zinc contaminated soil using phosphorus recovery product: hydroxyapatite/calcium silicate hydrate (HAP/C–S–H). Chemosphere. 2022;286:131664. https://doi.org/10.1016/j.chemosphere.2021.131664.
47. Cao X, et al. Immobilization of Zn, Cu, and Pb in contaminated soils using phosphate rock and phosphoric acid. J Hazard Mater. 2009;164(2):555–64. https://doi.org/10.1016/j.jhazmat.2008.08.034.